Effective Subgrade Coefficients for Seismic Performance Assessment of Pile Foundations

W.L. Tan , S.T. Song & W.S. Hung
National Chung-Hsing Unuversity, Taiwan, R.O.C.

15 WCEE
LISBOA 2012

SUMMARY:
The soil subgrade coefficients available in current practices are not suitable for assessing the performance of pile foundations under large deformation. The primary goal of this study is to determine the soil subgrade coefficients appropriate for limit state analysis of concrete piles. A set of modification factor is also obtained to modify the stiffness of the soil-pile system after the formation of the plastic hinge at the pile-head. Results indicate that the subgrade coefficient and stiffness modification factors suitable for limit state analysis of soil-pile systems is dependent on the soil properties as well as the reinforcement ratio and the above ground height of the pile. The outcome of the study is validated using finite element analysis of soil-pile systems. The comparison shows that the subgrade coefficient obtained in this study can reasonably estimate the lateral stiffness of soil-pile systems subjected to large deformation.

Keywords: pile foundation, subgrade coefficient, push-over analysis, soil-foundation interaction

1. INTRODUCTION

The seismic performance of bridge structures is significantly influenced by the strength and ductility of the foundation. Following the capacity design principle, the foundations of bridges are normally designed for a higher lateral strength, comparing the columns, to prevent undesired inelastic deformation occurring below the ground level. However, post-earthquake inspections in recent seismic events have suggested that pile foundations are highly susceptible to damage from earthquake load. Since the inelastic deformation of pile foundations may be difficult to avoid during a severe earthquake event, the non-linear behaviour of the soil-pile system must be carefully assessed, particularly if a certain level of performance is to be guaranteed for the structure.

For soil-pile system subjected to horizontal seismic motion, the large lateral loading may result in sequential yielding along the length of pile until a plastic mechanism is fully developed. Fig. 1.1 shows the deflected shape and the associated bending moment distribution at various limit states of a laterally loaded fixed-head pile. The first yield limit state of the pile, which is shown in Fig. 1.1(a), is characterized by a maximum bending moment at the pile/pile-cap connection where the flexure strength M_u of the pile is reached. A plastic hinge is then assumed to form at the pile head with the center of the rotation occurring at the ground level. Further displacement beyond the first yield limit state involves a concentrated rotation of the plastic hinge, which is accompanied by a redistribution of internal force in the pile. The redistribution increases the bending moment in the non-yielding portion of the pile until the formation of a second plastic hinge, as shown in Fig. 1.1(b). Continued lateral displacement after the second plastic hinge formation is facilitated by inelastic rotations in both plastic hinges until the pile reaches the ultimate limit state.

In current practices, many techniques are available to investigate the behaviour of pile foundations subjected to lateral loads. An acceptable and convenient approach is to analyze the laterally loaded soil-pile system as a flexural member supported by Winkler foundations. In such approach, the soil is

modelled as a series of springs with a constant stiffness, which is commonly characterized as the soil subgrade coefficient. Since most foundations are traditionally designed for elastic response, the subgrade coefficient available in current practices is intended for soil-pile system under small deformation and may not be suitable for analyzing the response of pile foundations reaching their yield limit. Moreover, pile deformation beyond the first yield limit state induces further softening of the surrounding soil and therefore significantly reduces the lateral stiffness of the soil-pile system. In order to carefully assess the performance of the pile foundations under large deformation, a set of subgrade coefficients and modification factors is obtained in this study. The subgrade coefficient is table for evaluating the effective stiffness of the soil-pile system at the first yield limit state. The reduced stiffness of the soil-pile system after the formation of the first plastic hinge is estimated by applying the modification factor into the solution of a flexural member on Winkler foundation model. In this study, the subgrade coefficients and modification factors are validated using the finite element analysis of soil-pile system. The result shows that the obtained coefficients can be used to reasonably estimate the stiffness of soil-pile system subjected to lateral deformation.

2. LATERAL LOAD-DISPLACEMENT RELATION OF SOIL-PILE SYSTEMS

The load-displacement relation and significant yield limit state of laterally loaded pile is illustrated in Fig. 2.1. The response can be further idealized as a tri-linear curve, characterized by an initial linear elastic response with a stiffness K_1, followed by a reduced stiffness K_2 due to a first yielding of the pile-head, and then by a fully plastic mechanism after the formation of the second plastic hinge. The first and second limit states are defined by the lateral yielding displacement Δ_{y1} and Δ_{y2}, respectively. The lateral force associated with the first and second yield limit state are denoted as V_y and V_u, respectively. Identifying the lateral loads and displacements at the two yield limit states allows the tri-linear load-displacement curve, as well as the stiffness of soil-pile system to be determined. In this paper, the lateral stiffness calculated using a flexural member on Winkler foundation model is compared with the lateral stiffness assessed by a computer simulation of a laterally loaded soil-pile system. The comparison provides the effective subgrade coefficient at the yield limit state of the soil.

3. LATERAL STIFFNESS OF SOIL-PILE SYSTEM

3.1. Cohesive Soils

3.1.1. Analytical approach
A common approach to estimate the lateral stiffness of a soil-pile system involves using the close-form solutions of a flexural member on elastic Winkler foundation model. For cohesive soils, the stiffness of the soil is assumed to be independent of the depth, resulting in a constant horizontal subgrade reaction k_h (in units of force/length^2). The governing equation of the model is given by: (Poulos and Davis, 1980)

$$EI_e \frac{d^4 y}{dx^4} + k_h y = 0 \qquad (3.1)$$

where EI_e is the effective flexural rigidity of the pile, y is the lateral deflection of the pile, and x is the depth below the ground surface. In order to solve the governing Eqn. 3.1, the characteristic length of the soil-pile system is first defined as:

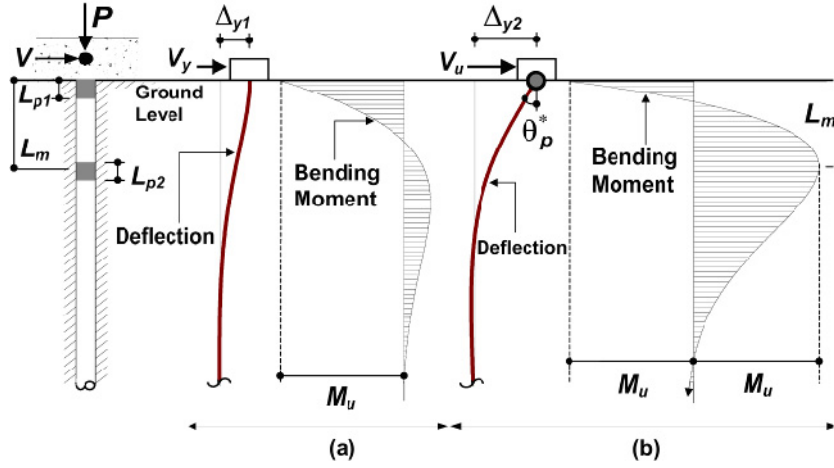$$R_c \equiv \sqrt[4]{\frac{EI_e}{k_h}} \qquad (3.2)$$

Figure 1.1. Deflected shape and bending moment distribution of a fix-head pile loaded at the ground level (a) first limit state and (b) second limit state
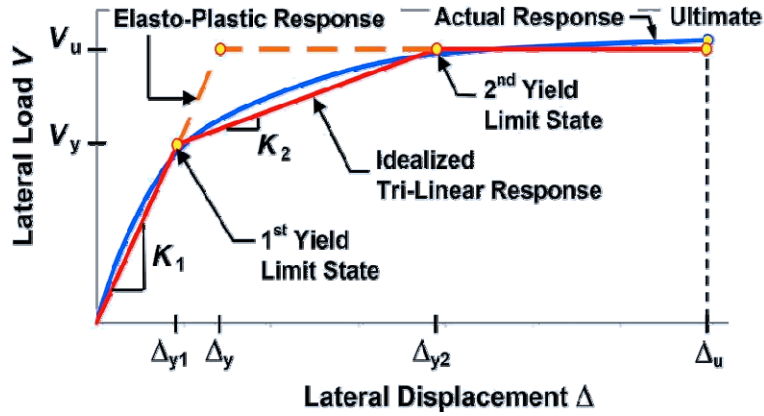

Figure 2.1. Idealized load-displacement curve and significant limit states of laterally loaded piles

The solution of Eqn. 3.1, in conjunction with appropriate boundary conditions, and the idealized initial stiffness K_1 of piles with a rotational restraint at the pile-head is given by: (Song, 2005)

$$K_1 = \frac{V_y}{\Delta_{y1}} = \frac{12}{6\sqrt{2} + 6\xi_a + 3\sqrt{2}\xi_a^2 + \xi_a^3} \frac{EI_e}{R_c^3} \tag{3.3}$$

where Δ_{y1} and V_y are the lateral displacement and the lateral force at the first yield limit state, EI_e is the effective flexural rigidity of the pile, and $\xi_a = L_a / R_c$ is the above ground height coefficient, defined as the above ground height L_a of the pile normalized by the characteristic length R_c of the soil-pile system. After the formation of the first plastic hinge, the idealized post-yield stiffness K_2 of the soil-pile system could be obtained by:

$$K_2 = \frac{V_u - V_y}{\Delta_{y2} - \Delta_{y1}} = \frac{3}{3\sqrt{2} + 6\xi_a + 3\sqrt{2}\xi_a^2 + \xi_a^3} \frac{EI_e}{R_c^3} \tag{3.4}$$

where Δ_{y2} is the lateral displacement at the second yield limit state, and V_u is the lateral force at the second yield limit state. The lateral stiffness K_1 and K_2, as characterized in Eqn. 3.3 and Eqn. 3.4, require the determination of the characteristic length R_c of the pile, which in turn requires an estimation of the modulus of horizontal subgrade reaction k_h. In current practices, the value of k_h is commonly estimated based on the undrained shear strength s_u of cohesive soils. An expression for

k_h is proposed by Davisson (1970), i.e.:

$$k_h = 67\, s_u \tag{3.5}$$

where s_u is the undrained shear strength of the cohesive soil, which may be determined from field tests or be estimated directly from site classifications in current building codes.

3.1.2. Computer simulation

In this study, the non-linear behaviour of a soil-pile system subjected to lateral loads is simulated using the computer program LPILE (Reese et al, 2004). The soil pressure induced by pile deformation is given by the non-linear p-y relations widely used in geotechnical engineering practices. For cohesive soils, the p-y relation proposed by Matlock (1970) is used. The pile is modeled as a flexural member with its flexural rigidity and moment-curvature relation of the pile section specified. Outcomes of the simulation gives the lateral load-displacement relations at the first yield limit state, denoted as V_y and Δ_{y1}, and at the second yield limit state, denoted as V_u and Δ_{y2} in Fig. 2.1. To this end, the initial stiffness K_1 can be calculated by $K_1 = V_y / \Delta_{y1}$ and the post-yield stiffness K_2 is given by $K_2 = (V_u - V_y)/(\Delta_{y2} - \Delta_{y1})$.

In order to estimate the effective subgrade coefficient at the first yield limit state, the initial stiffness K_1 estimated by the simulation is first substituted into Eqn. 3.3 to calculate the characteristic length R_c of the soil-pile system. The effective subgrade coefficient $\bar{k}_h$ can then be determined using Eqn. 3.2. As mentioned earlier, pile deformation beyond the first yield limit state induces further softening of surrounding soil. The soil softening affects the characteristic length of the soil-pile system and therefore reduces the post-yield stiffness. To evaluate the effect of soil softening due to the large deformation after the first yield limit state, the post-yield stiffness K_2 suggested by the simulation is compared with Eqn. 3.4 from the analytical model. A modification factor κ_c can then be introduced to modify the characteristic length for estimating the post-yield stiffness of soil-pile systems. More specifically, the modified characteristic length $\kappa_c R_c$, denoted as the characteristic length R_c multiplied with a modification factor, is give by reorganizing Eqn. 3.4 to:

$$\kappa_c R_c = \sqrt[3]{\frac{3}{3\sqrt{2} + 6\xi_a + 3\sqrt{2}\xi_a{}^2 + \xi_a{}^3} \frac{EI_e}{K_2}} \tag{3.6}$$

where ξ_a is the above ground height coefficient, EI_e is the effective flexural rigidity of the pile, and K_2 is the reduced stiffness suggested by the simulation.

3.2. Cohesionless Soils

3.2.1. Analytical approach

Like cohesive soils, a similar approach to estimate the lateral stiffness of a soil-pile system involves using the close-form solutions of a flexural member on elastic Winkler foundation model. For cohesionless soils, the stiffness of the soil is assumed to be the constant rate of increase of the horizontal subgrade reaction, and may be defined as $n_h = k_h / x$ (in units of force/length^3). The governing equation of the model is given by: (Poulos and Davis, 1980)

$$EI_e \frac{d^4 y}{dx^4} + n_h x y = 0 \tag{3.7}$$

where EI_e is the effective flexural rigidity of the pile, y is the lateral deflection of the pile, and x is the depth below the ground surface. The characteristic length of the soil-pile system is used to solve Eqn. 3.7, and defined as following equation.

$$R_n \equiv \sqrt[5]{\frac{EI_e}{n_h}} \qquad\qquad (3.8)$$

From solving Eqn. 3.7 with appropriate boundary conditions, the idealized initial stiffness K_1 of piles with a rotational restraint at the pile-head is given by: (Song, 2005)

$$K_1 = \frac{V_y}{\Delta_{y1}} = \frac{1}{0.94 + 0.86\xi_a + 0.44\xi_a{}^2 + 0.083\xi_a{}^3} \frac{EI_e}{R_n{}^3} \qquad (3.9)$$

where V_y and Δ_{y1} are the lateral force and the lateral displacement at the first yield limit state, EI_e is the effective flexural rigidity of the pile, and $\xi_a = L_a / R_n$ is the above ground height coefficient, defined as the above ground height L_a of the pile normalized by the characteristic length R_n of the soil-pile system. From the first limit state to second limit state, the idealized post-yield stiffness K_2 of the soil-pile system could be developed by:

$$K_2 = \frac{V_u - V_y}{\Delta_{y2} - \Delta_{y1}} = \frac{3}{7.29 + 9.71\xi_a + 5.24\xi_a{}^2 + \xi_a{}^3} \frac{EI_e}{R_n{}^3} \qquad (3.10)$$

where V_u is the lateral force at the second yield limit state, and Δ_{y2} is the lateral displacement at the second yield limit state. Using Eqn. 3.9 and Eqn. 3.10 to evaluate the lateral stiffness K_1 and K_2, require the determination of the modulus of the horizontal subgrade reaction n_h, which used to estimate the characteristic length R_n of the soil-pile system for chesionless soils. In current practices, the value of n_h is commonly estimated based on the friction angle ϕ of cohesionless soils. An expression for n_h is proposed by ATC-32(1996), as shown in Fig. 3.1.
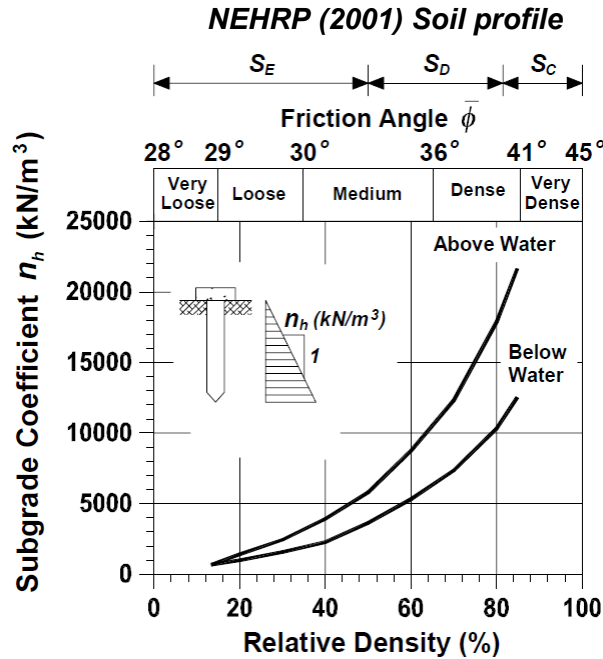

Figure 3.1. Subgrade coefficients of cohesionless soils recommended by ATC-32(1996)

3.2.2. Computer simulation

Like cohesive soils, the non-linear behaviour of a soil-pile system subjected to lateral loads is simulated using the computer program LPILE (Reese et al, 2004). The pile is modeled as a flexural member with its flexural rigidity and moment-curvature relation of the pile section specified. The soil pressure induced by pile deformation is given by the non-linear p-y relations used in geotechnical engineering practices. For cohesionless soils, the p-y relation proposed by API (1993) is used. Outcomes of the simulation gives the lateral load-displacement relations at the first yield limit state, denoted as V_y and Δ_{y1}, and at the second yield limit state, denoted as V_u and Δ_{y2} in Fig. 2.1. For the purpose in the study, the initial stiffness K_1 can be calculated by $K_1 = V_y / \Delta_{y1}$, and the post-yield stiffness K_2 is given by $K_2 = (V_u - V_y)/(\Delta_{y2} - \Delta_{y1})$.

As with cohesive soils, in order to estimate the effective subgrade coefficient at the first yield limit state, the initial stiffness K_1 estimated by the simulation is first substitute into Eqn. 3.9 to calculate the characteristic length R_n of the soil-pile system. Using Eqn. 3.8, the effective subgrade coefficient $\bar{n}_h$ can then be obtained. Additionally, surrounding soil became soften because of pile deformation beyond the first yield limit state. The soil softening influences the characteristic length of the soil-pile system and therefore reduces the post-yield stiffness. In order to assess the influence of soil softening due to the large deformation after the first yield limit state, the post-yield stiffness K_2 obtained by the simulation is compared with Eqn. 3.10 from the analytical model. A modification factor κ_n can be developed to modify the characteristic length for evaluating the post-yield stiffness of soil-pile systems. Like the cohesive soil, the modified characteristic length $\kappa_n R_n$, denoted as the characteristic length R_n multiplied with a modification factor, is give by reorganizing Eqn. 3.10 to:

$$\kappa_n R_n = \sqrt[3]{\frac{3}{7.29 + 9.71\xi_a + 5.24\xi_a{}^2 + \xi_a{}^3} \frac{EI_e}{K_2}} \qquad (3.11)$$

where ξ_a is the above ground height coefficient, EI_e is the effective flexural rigidity of the pile, and K_2 is the reduced stiffness suggested by the simulation.

4. SUBGRADE COEFFICIENTS AND MODIFICATION FACTORS

Twenty-seven piles with different diameters D, longitudinal steel ratios ρ_L and above ground heights L_a are considered for the study. The undrained shear strength s_u of the soil is taken to vary from 20 kPa for soft clays to 200 kPa for very stiff clays. The friction angle ϕ of the soil is taken to vary from $29°$ for soft sands to $42°$ for very stiff sands. The correlation between the effective soil subgrade coefficient $\bar{k}_h$ and the undrained shear strength s_u is illustrated in Fig. 4.1(a). For comparison, the subgrade coefficient given by Eqn. 3.5 is also shown in the figure. It can be seen from the figure that the effective subgrade coefficient increases with the increasing undrained shear strength of the soil. The subgrade coefficients suggested by the p-y curves are significantly larger than those calculated from Eqn. 3.5 for medium and stiff clays. The correlation between the effective soil subgrade coefficient $\bar{n}_h$ and the friction angle ϕ is illustrated in Fig. 4.1(b). For comparison, the subgrade coefficient given by ATC-32 (1996) is also shown in the figure. Additionally, the subgrade coefficients suggested by the p-y curves are significantly smaller than those calculated from ATC-32 (1996) for medium and stiff sands. Note that since the effective subgrade coefficient is correlated to the yield limit state of the pile element, the value of the subgrade coefficient is related to the longitudinal steel ratio and above ground height of the pile. For a given undrained shear strength or friction angle, the subgrade coefficient for piles with low longitudinal steel ratios is larger than that for piles with high longitudinal steel ratios. Additionally, the subgrade coefficient increases with the increasing above ground height. However, for a given undrained shear strength or friction angle, piles with the same longitudinal steel ratios and above ground height tend to have similar subgrade

coefficients for all diameters.

Fig. 4.2(a) shows the correlation between the modification factor κ_c and the undrained shear strength s_u of cohesive soils. The modification factor κ_c decreases with increasing undrained shear strength. Fig. 4.2(b) shows the correlation between the modification factor κ_n and the friction angle ϕ of cohesionless soils. The modification factor κ_n decreases with increasing friction angle for stiff sand and increases with increasing friction angle for soft sand. Additionally, the value of κ_c or κ_n is depended on the above ground height but only slightly influenced by the longitudinal steels ratio ρ_L. It can also be seen from Fig. 4.2 that all modification factors are greater than unity, indicating an increase in characteristic length or a further decrease of lateral stiffness.
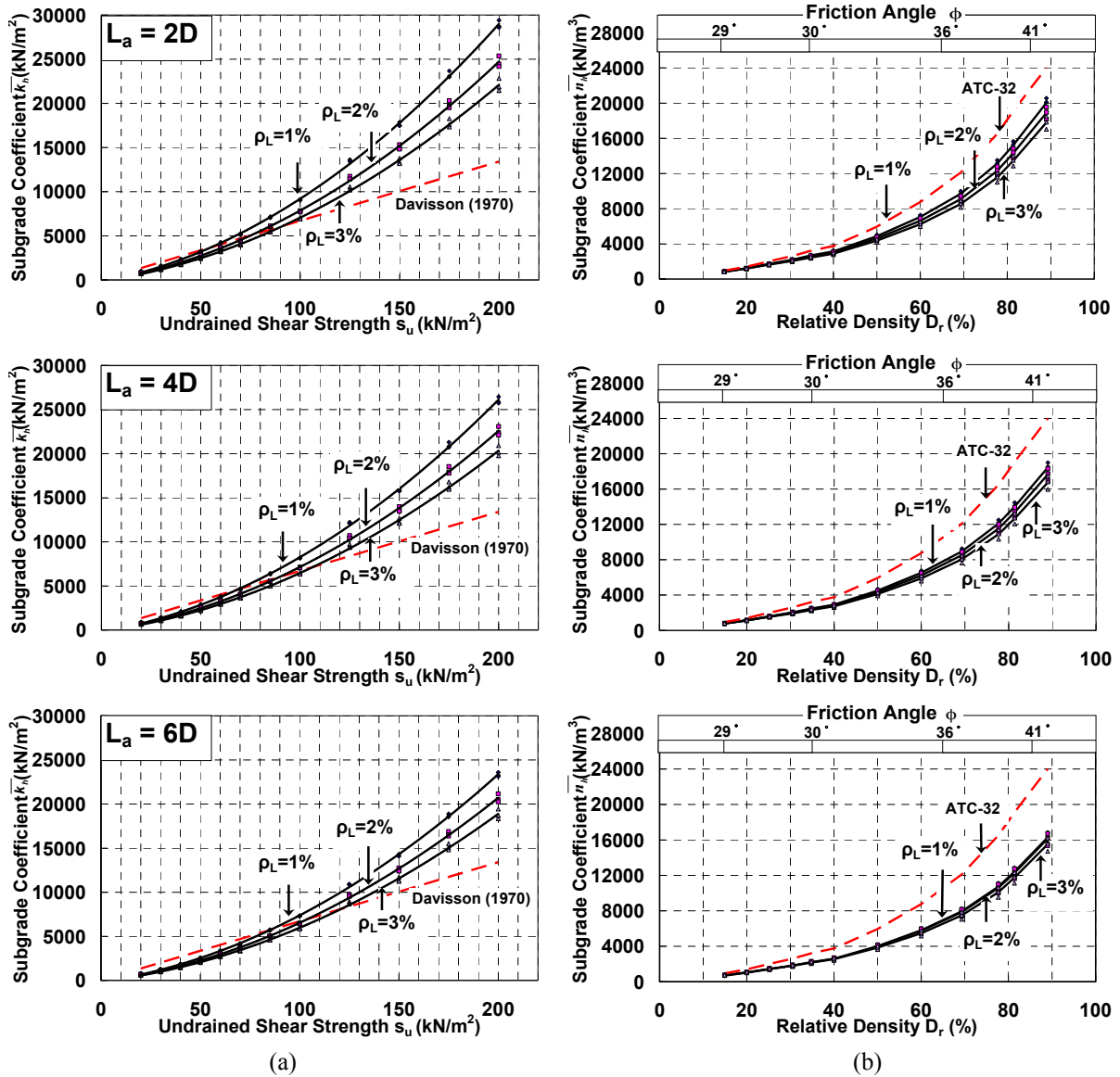

(a)   (b)

Figure 4.1. Effective subgrade coefficient for piles with different above ground heights
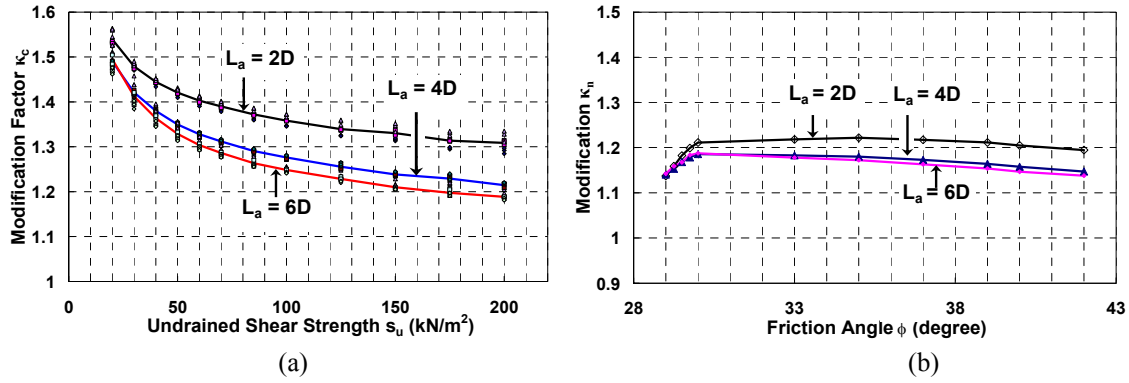(a) cohesive soils and (b) cohesionless soils

Figure 4.2. Characteristic length modification factors for (a) cohesive soils and (b) cohesionless soils

5. COMPARISON WITH FINITE ELEMENT MODEL

In order to ensure the confidence in the applicability of the effective subgrade coefficient, the tri-linear load-displacement relationship from the analytical model is compared with the pile response predicted by the finite element analysis. The analytical model has been adjusted with the effective subgrade, the stiffness coefficient $\bar{k}_h$ or $\bar{n}_h$, and the post-yield modification factor κ_c or κ_n. The finite element analysis is carried out using the analysis platform OpenSees (McKenna et al, 2008). The general schematic of the finite element model is shown in Fig. 5.1. In the model, the pile section is the fiber section, and the resistance of the soil is modeled by the non-linear p-y springs proposed by Matlock (1970) for cohesive soils and API (1993) for cohesionless soils.

To illustrate the method outlined in this paper, consider an extended pile-shaft with a diameter of $D = 0.91\,\text{m}$, the effective flexural rigidity of $EI_e = 446400\ \text{kN-m}^2$, and the longitudinal steel ratio of $\rho_L = 2\%$. The above ground heights L_a are $2D$, $4D$, and $6D$. The property of the soils is summarized in Table 5.1. And the results are shown in Fig. 5.2. The data for the comparison with cohesive soil is illustrated in Fig. 5.2(a). It can be seen from the figure that the tri-linear load displacement relation given by the analytical model with the modified soil stiffness compares well with the response from the finite element analysis. The analytical model is able to capture the initial secant stiffness of the soil-pile system prior to the first yield limit state. The post yield stiffness predicted from the analytical model also tracks well the slope of the load-displacement curve of the finite element model well, the ultimate strength estimated by both models is in close agreement with each other.

The data for the comparison of cohesionless soil is illustrated in Fig. 5.2(b). The analytical model, again, is able to capture the initial secant stiffness of the soil-pile system before the first yield limit state. The post yield stiffness predicted from the analytical model paths well the slope of the load-displacement curve from the finite element model for the soft sand. However, the ultimate strength evaluated by both models is really different with each other. The reason is that the p-y relations proposed by different approach in the two models. The ultimate soil pressure recommended by API (1993), which is used for the soil elements in the finite element model, is significantly larger than that proposed by Broms (1964), which is adopted in the kinematic model.

Table 5.1. The properties of soils

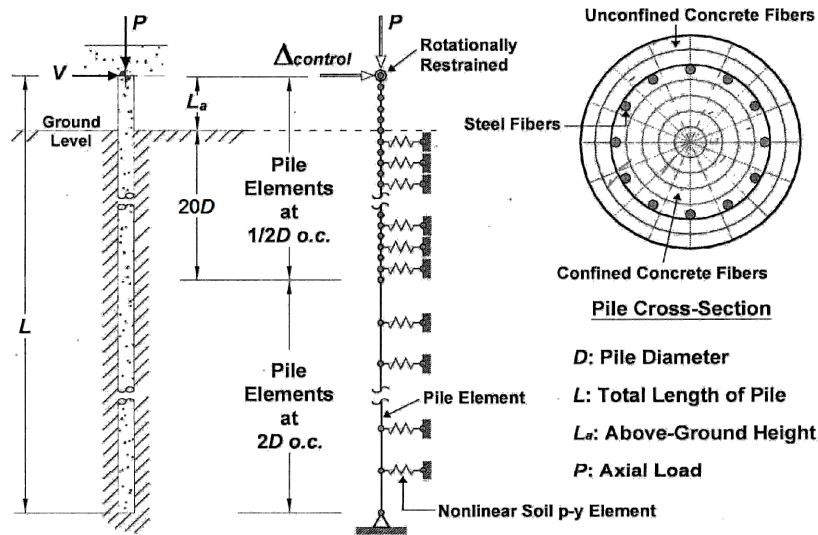| Soil type	Soil property	S_E	S_D	S_C
Cohesive soils	Effective unit weight γ' (kN/m^3)	15.5	17.5	18.5
	Undrained shear strength s_u (kN/m^2)	40	85	125
Cohesionless soils	Effective unit weight γ' (kN/m^3)	17	18.5	20
	Friction angle ϕ (degree)	31	37	42

Figure 5.1. General schematic of the finite element model for laterally loaded fixed-head concrete piles
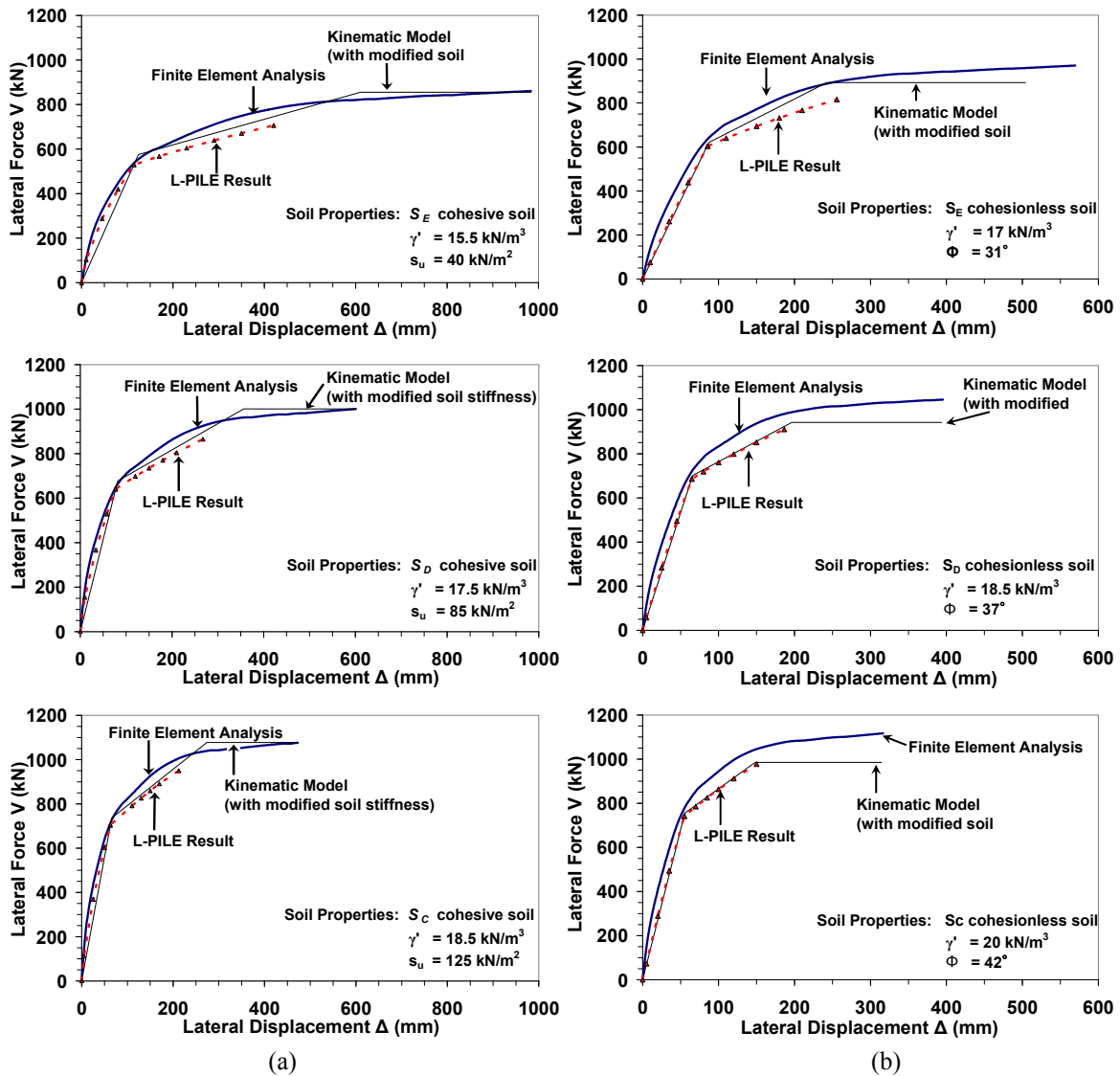

Figure 5.2. Comparison of the lateral load-displacement responses of soil-pile systems
(a) cohesive soils and (b) cohesionless soils

6. CONCLUSIONS

During a severe earthquake, the inelastic deformation of pile foundations may be difficult to avoid. In order to carefully assess the nonlinear behaviour of laterally loaded soil-pile system, a set of effective subgrade coefficients, which correlated to the yield limit state of the pile, is obtained in this study. Results of the study show that the value of the effective subgrade coefficient is dependent on the longitudinal steel ratio and above ground height of the pile. Another set of modification factors is also calculated to adjust the characteristic length and modify the post-yield stiffness of the soil-pile system. The value of the modification factors are also related to above ground height of the pile. The outcomes obtained in this study are validated using the finite element analysis. For cohesive soils, the result indicates that with the modified soil stiffness, equations provided by the beam on Winkler foundation model are capable of capturing the stiffness of a soil-pile system subjected to a large lateral demand. For cohesionless soils, the initial stiffness predicted from the analytical model is able to capture the initial scent stiffness of the soil-pile system. However, the ultimate strength provided by the analytical model is really different from the ultimate strength proposed by finite element model. The reason is that the p-y relations of the two models are recommended by different approach. Actually, it means that the effective subgrade coefficients provided from this study can be used well to evaluate the first limit state of soil-pile systems subjected to a large deformation.

REFERENCES

American Petroleum Institute API. (1993). API Recommended Practice for Planning, Designing and Constructing Fixed Offshore Platforms, API Recommended Practice 2A (RP2A), Twentieth edition, Washington D.C.

Applied Technology Council ATC-32. (1996). Improved Seismic Design Criteria for California Bridges：Provisional Recommendations, Redwood City, California.

Broms, B. B. (1964). Lateral resistance of piles in cohesionless soils. Journal of the Soil Mechanics and Foundations Division, American Society of Civil Engineering, VOL.90: SM3, pp.123-156.

Davisson M. T. (1970). Lateral load capacity of piles, Highway Research Record, NO.333, pp. 104-112.

Matlock H. (1970). Correlation for design of laterally loaded piles in soft clay. Proceedings, 2nd Annual Offshore Technology Conference, OTC 1204(1), Houston, Texas.

McKenna F., Fenves G. L., Jeremic B. and Scott M.H. (2008). Open System for Earthquake Engineering Simulation, <http://opensees.berkeley.edu>.

NEHRP. (2001) NEHRP recommended provisions for seismic regulations for new buildings and other structures, FEMA 368. Washington, D.C.

Poulos H. G. and Davis E. H. (1980). Pile Foundation Analysis and Design, Willey-Interscience, New York.

Reese L. C. , Wang S. T. , Isenhower W. M., Arrellaga J. A. and Hendrix J. (2004). LPILE Plus Version 5.0-A Program for the Analysis of the Piles and Drilled shafts under Lateral Loads. Ensoft, Inc Austin Texas.

Song S. T. (2005). Limit State Analysis and Performance Assessment of Fixed-Head Concrete Piles under Lateral Loading, PH.D. Thesis University of California, Davis.